UNIVERSITY OF NAPLES FEDERICO II

PH.D. PROGRAM IN

CLINICAL AND EXPERIMENTAL MEDICINE

CURRICULUM IN (CARDIOVASCULAR AND GERONTOLOGICAL SCIENCES)

XXX Cycle
(Years 2014-2017)

Chairman: Prof. Gianni Marone

PH.D. THESIS

TITLE

β-arrestin 2 deletion improves cardiac function during aging

TUTOR	PH.D. STUDENT
Prof. Nicola Ferrara	**Dr. Claudio de Lucia**

INDEX

BACKGROUND

Over the last years, life expectancy has significantly increased although multiple diseases persist with aging as a risk factor. In fact, despite the improvement in treatments, many elderlies suffer from cardiovascular diseases(1). The pathophysiological changes of the aging heart include left ventricular (LV) hypertrophy, diastolic and systolic dysfunction, increased fibrosis and reduced inotropic reserve(2-4). These changes make aged heart more vulnerable to stress, leading to a high prevalence of cardiac diseases such as arrhythmias, coronary artery disease, myocardial infarction and heart failure (HF) (1, 5). All these alterations are mirrored in animal models used in aging studies. In particular, the application of genetically modified mice to aging research has identified numerous critical molecular mechanisms involved in cardiac aging such as altered adrenergic signaling, mitochondrial dysfunction, increased cardiomyocyte apoptosis and oxidative stress(2, 6, 7). β-arrestin-1 (βarr-1) and βarr-2 proteins belong to the arrestin family and are ubiquitously expressed. They have been originally discovered as regulators of the G protein–coupled receptor (GPCR) signaling but both are now well known to be also G protein–independent signal transducers and interact with many proteins and protein kinases both in vitro and in vivo(8, 9). In the cardiomyocytes, when β-adrenergic receptors (β-ARs) are stimulated by catecholamines, the G protein-coupled receptor kinase 2 (GRK2) phosphorylates β-ARs that then become targets for the binding of β-arrs. This β-arr binding prevents β-ARs further coupling to the G protein, reduces the level of functional receptors and induces their internalization where they go on to be degraded or resensitized before recycling to the membrane(10). It is well established that GRK2 is upregulated in failing heart leading to β-AR dysfunctional signaling(10).

Differently, cardiac membrane GRK2 levels are not altered with aging and the main mechanism involved in the age–related β-AR down-regulation/desensitization in cardiomyocytes remains still unknown(11). Interestingly, β-arr-2 protein levels are increased in the aged heart(12). However it is not clear so far if β-arr-2 plays a role in the decreased adrenergic signaling during cardiac aging. Thus, in the present study we have tested the effects of β-arrestin-2 deletion in a murine model of aging on cardiac function and age-related β-AR dysfunction.

METHODS

Experimental animals

All animal procedures were performed in accordance with the guidelines of the Institutional Animal Care and Use Committee of Temple University School of Medicine. Genetically engineered, β-arr2 KO (on C57BL/6 background) and corresponding C57BL/6 wild type (WT) male mice were used for this study, as previously published(13). All animals were bred and maintained on a C57Bl/6 background. Mice were studied for a 15-24-month-long period according to different experiments.

Two-Dimensional Echocardiography and Strain Analysis

Transthoracic echocardiography has been used to assess cardiac structure and function using a VisualSonics VeVo 2100 system (VisualSonics, Toronto, Ontario, Canada), as described. Mice were anesthetized in a specific isoflurane sedation box (induction 3.0% and maintenance 1–3%). Mice were next shaved to remove hair from the ventral thorax (from the neckline to mid-chest level). Then, mice were placed in a supine position on a heated table with embedded ECG leads. During echocardiography, anesthesia was maintained throughout the procedure with 1–3% isoflurane. Images were acquired in the short-axis B-mode and M-mode for LV diameters, anterior and posterior wall measurements, and subsequently ejection fractional (EF) with a 18–38 MHz probe(14, 15).

Long-axis B-mode images were recorded for endocardial longitudinal and radial strain as well as longitudinal strain rate (SR) and radial SR analysis using the Vevo Strain software following, as published(14, 16). Strain, which evaluates change in length relative to the initial length (Strain = Final Length [L]/ Initial Length [L0]) was calculated either in the radial (from the center of the ventricle cavity outward) or longitudinal axis (from the apex to the base). The rate of change in strain (Strain Rate = Strain/Time) was also measured(14). Average and regional (6 segments: anterior basal zone, anterior middle zone, anterior apex, posterior basal zone, posterior middle zone, posterior apex) LV endocardial longitudinal and radial strain/SR were evaluated(16, 17). After echocardiograms were recorded, image series were randomly ordered and renumbered. All images were analyzed under their coded numbers in a blinded fashion, then the code was broken and animal data was sorted by treatment group then analyzed.

Membrane Preparation and Radioligand Binding

β-AR density was measured in isolated cardiac plasma membranes using ^{125}I-CYP (Iodocyanopindolol), as described(18). Membrane preparations from LV samples were prepared by homogenization in ice-cold lysis buffer (25 mM Tris, pH 7.4, 5 mM EDTA, 1 μg/mL aprotinin, 1 μg/mL leupeptin) and centrifuged at 1,000 × g for 5 min at 4 °C. The supernatant was centrifuged at 30,000 × g, and the crude membrane pellet was resuspended in lysis buffer containing 10% glycerol and stored at −80 °C until use. The density of βAR on membranes was determined by saturation binding experiments. Membrane preparations (25 μg of protein) were incubated with [^{125}I]cyanopindolol ([^{125}I]CYP; 200 pM; PerkinElmer) in binding buffer (75 mM Tris, pH 7.4, 2 mM EDTA, 12.5 mM MgCl2, 1 μg/mL aprotinin, 1 μg/mL leupeptin). Incubations were performed in the presence or absence of propranolol (10 μM) to determine nonspecific binding. The reactions were performed in a 250-μL volume and allowed to equilibrate at 37 °C for 1 h before filtering the membranes through a glass fiber filter (Whatman GF/C; Brandel). Each filter was washed five times with 5 mL of ice-cold wash buffer (10 mM Tris, pH 7.4, 10 mM EDTA) to remove unbound drug. The amount of total and non-specific radiolabel bound to cell membranes was determined on a gamma counter. All assays were performed in triplicate. Receptor density was normalized to milligrams of membrane protein.

Western blot analysis

Western blotting has been performed as published(15). LV samples (0.1 mg) were lysed in a RIPA buffer with protease (cOmplete-Roche, Indianapolis, IN, USA) and phosphatase inhibitors (PhosSTOP-Roche, Indianapolis, IN, USA) cocktail. Protein content was quantified with the Bio-Rad BCA protein assay (Bio-Rad Laboratories, Richmond, California, USA). Protein samples were separated by 4–20% SDS–polyacrylamide gel electrophoresis (Thermo Fisher Scientific) and then transferred to nitrocellulose membrane (Bio-Rad Laboratories). After blocking with a specific blocking buffer (Odyssey, LI-COR, Lincoln, Nebraska, USA), the membranes were incubated and probed with the first antibody at 4 °C overnight according to manufacturer's instructions. Then, the proteins were stained with a corresponding Alexa Fluor 680- (1:5,000; Thermo Fisher Scientific) or IRDye 800CW-coupled (1:5,000; Rockland Inc. Limerick, PA, USA) secondary antibody, followed by visualization of the proteins with a LI-COR infrared imager (Odyssey), and quantitative densitometric analysis was performed applying Odyssey version 1.2 infrared imaging software. Protein levels of: β-arr2 (Santa Cruz

sc-13140; 1:1,000); NOX4 (Epitomics #3187-1; 1:1,000), Mn-SOD (BD-Biosciences #611580; 1:1,000) were assessed.

Real-time PCR and RT-PCR

Total RNA was isolated from LV specimens with TRIzol (Thermo Fisher Scientific) according to the company's instructions. After RNA isolation, cDNA was synthesized by reverse transcription of the RNA (iScript cDNA synthesis kit, Bio-Rad Laboratories). Real-time PCR was performed in triplicates on a CFX96 real-time PCR detection system (Bio-Rad Laboratories) using the SYBR Green mix (Bio-Rad Laboratories) and specific primers for mouse β-arr1 as follows: forward 5'-AAGGGACACGAGTGTTCAAGA-3'; reverse 5'-CCCGCTTTCCCAGGTAGAC-3';

β-arr2 as follows: forward 5'-GGCAAGCGCGACTTTGTA-3'; reverse 5'-GTGAGGGTCACGAACACTTTC-3'(19). The expression levels were normalized to the rRNA 18S. Specificity of PCR products was confirmed by melting curve and gel electrophoresis(15).

Conventional RT-PCR for the presence of β-arr2 transcript in mRNA extracted from LV samples was performed with specific primers for mouse β-arr2 as follows: forward 5'-AAGTCGAGCCCTAACTGCAA-3'; reverse 5'-TTCCGGTCCTTCAAGTAGTCA-3'

RESULTS

β-arr2 mRNA expression and protein levels in aging hearts

To confirm that aging is associated with increased β-arr2 in the heart(12), we measured LV β-arr2 protein levels in young and old mice. There was a 2.7 fold increase in β-arr2 protein levels in 15- versus 6-month-old WT-mice (p<0.0001) (Fig. 1B). Differently, we found similar mRNA expression of β-arr2 in samples from 15- versus 6-month-old mouse hearts (Fig. 1A).

β-arr2 deletion did not affect neither β-arr1 cardiac expression nor age-related cardiac hypertrophy

In order to investigate the impact on cardiac aging of the genetic deletion exclusively of β-arr2, we utilized the available global β-arr2 KO mouse model (Figure 2A). These mice breed normally and did not present any basal altered cardiovascular phenotype(13). β-arr2 KO-Old mice did not show different β-arr1 expression when compared to WT-Old mice (Figure 2B). As expected, aging in WT mice was associated with increase in body weight (BW) (6- vs 24

5

month-old: 23±0.65 vs 33±0.87), heart weight (HW) (6- vs 24 month-old: 0.12±0.0032 vs 0.17±0.0036), and HW to tibia length ratio (HW/TL) (6- vs 24 month-old: 7±0.19 vs 9.3±0.18) (Figure 3, Table). Interestingly, when compared to WT-Old mice, β-arr2-KO Old mice did not show any changes in BW (33±0.87 vs 32±0.79), HW (0.17±0.0036 vs 0.18±0.0063), HW/BW (5.2±0.18 vs 5.5±0.2), HW/TL (9.3±0.18 vs 9.5±0.34) (Figure 3, Table). β-arr2 deletion did not affect BW, HW, HW/BW or HW/TL in young (6-month-old) mice, as well (Figure 3, Table).

β-arr2KO deletion improves cardiac function during aging

There were no differences between groups (β-arr2 vs. WT) in any of the echocardiographic measures (standard echocardiography) when mice were 6-month-old (Figure 4 and Table). Aging was associated with a decline in LV EF (6-month-old: 57±1.3; 20-month-old: 49±1.3) as well as increased LV internal end-diastolic diameter (LVIDd) (6-month-old: 4.1±0.054; 20-month-old: 4.5±0.066), LV internal end-systolic diameter (LVIDs) (6-month-old: 3.0±0.053; 20-month-old: 3.5±0.067), and LV mass of the anterior wall (LV Mass AW) (6-month-old: 114±3.9; 20-month-old: 136±6) (Figure 4 and Table).

β-arr2KO deletion in old mice resulted in blunted age-related cardiac dysfunction. In fact, β-arr2KO 20-month-old mice, when compared to WT 20-month-old mice, showed increased EF (49±1.3 vs 57±1.8; p<0.01) as well as reduced LVIDd (4.5±0.066 vs 4.2±0.067; p<0.01) and LVIDs (3.5±0.067 vs 3.1±0.11; p<0.01) (Figure4 and Table). No difference was found in LV mass AW between the Old groups (β-arr2KO-Old vs WT-Old: 136±6 vs 136±9.7).

Strain analysis was performed on long-axis B-mode images to check longitudinal and radial strain parameters. When young, β-arr2KO and WT mice demonstrated similar average longitudinal and radial strain as well as average longitudinal SR and radial SR (Figure 5 A, C, E, G). Average Radial strain and radial SR were reduced while average longitudinal strain and longitudinal SR were not affected during aging in WT mice (Figure 5). Significant improvements in both average radial strain and radial SR were observed in β-arr2-KO Old when compared to WT-Old mice (p<0.05) (Figure 5B, D, F, H)

In addition, β-arr2 deletion improved regional radial and radial SR in the anterior basal zone and posterior apex during aging (p<0.05) (Figure 6 B, D). No differences were found in average and regional longitudinal strain and longitudinal SR between β-arr2-KO Old and WT-Old mice (Figure 5 B, D and Figure 7 B, D)

β-arr2KO deletion restored age-influenced cardiac β-AR density

In an effort to explore the molecular mechanisms underlying the effect of the absence of β-arr2 on cardiac function during aging, we also investigated β-AR density in β-arr2 and WT mice both when young and old. Consistent with the functional data, total β-AR density in the aged WT (24-month-old) hearts was reduced compared to WT young (6-month-old) hearts (WT-Young vs WT-Old: 79±2 vs 62±6.8 fmol/mg protein) (Figure 8). Importantly, β-arr2 deletion restored age-dependent β-AR downregulation ($p<0.05$) (WT-Old vs β-arr2-Old: 62±6.8 vs 84±7.2) (Figure 8). No difference was found between young groups in term of cardiac β-AR density (Figure 8).

β-arr2KO deletion reduced age-determined Nox4 upregulation

We confirmed that cardiac Nox4 is upregulated during aging[20] (increase of 3.7 fold in WT-Old compared to WT-Young; *$p<0.001$) and discovered that MnSOD is unchanged and probably is not able to metabolize enough ROS produced determining increased oxidative stress. (Figure 9 A, B). Intriguingly, we found that Nox4 was significantly down-regulated in βarr-1 KO- and βarr-2 KO-Old mice compared to WT-Old mice (respectively 40% and 30% decrease vs WT-Old; respectively $p<0.0001$ and $p<0.01$ vs WT-Old) while Mn-SOD values were similar in cardiac samples from old groups.

DISCUSSION

In the present study, we have demonstrated that βarr-2 deletion in aged mice is able to: a) improve age-related cardiac dysfunction b) enhance average and regional cardiac radial strain as well as radial SR during in aging heart c) restore age-related cardiac β-AR desensitization d) reduce cardiac oxidative stress.

Cardiovascular diseases impose a huge social, economical and clinical burden worldwide. The aging of the population in combination with increased survival in patients with coronary artery disease, hypertension, diabetes and arrhythmias has led to a tremendous growth in both the prevalence and incidence of HF[1, 21]. Therefore, there is an enormous need to invest in treatments contributing to a successful aging and increasing the quality of life. A lot of investments and efforts have been spent in the last decades in order to counteract the development and progression of cardiovascular diseases. Considerable advances in pharmacological treatment of HF have been achieved but researchers have not been focusing enough on cardiac age-related alterations (22). This is crucial since a frail heart is more prone to develop cardiac dysfunction after stress (myocardial infarction, hypertension, diabetes,

etc.). Unfortunately, the basic mechanisms that cause the aging of the heart are still poorly understood. Age-related cardiac modifications are represented by cardiomyocyte hypertrophy, increased myocardial thickness and cardiac fibrosis, which together affect LV structure and function(2). Many studies have shown that the aging is characterized by changes of β-AR system such as increased plasma catecholamine levels, reduction of cardiac receptor density and their internalization as well as decreased adenylyl cyclase activity and cAMP production(6, 12, 23). Cardiac β-AR dysfunction during aging leads to reduced exercise tolerance, decreased LV inotropic reserve and less susceptibility to β-blockade compared to young people(6). Although changes in β-AR agonist responsiveness in the failing and aging heart are quite similar, GRKs expression and activity seem to be unaltered during aging(24, 25). Hence, the main molecular mechanism involved in β-AR dysfunction during aging is still undetermined. Interestingly, Dobson et al. studied potential molecular mechanisms of reduced β-AR signaling in the aged heart and found β-arr2 to be upregulated despite β-arr2 is known to be less expressed compared to β-arr1 in the heart(12, 26). In addition, a recent study elucidated the phosphorylation site of the β1-AR at Ser461/Ser462 in the distal part of the C-terminus to determine β-arr2 recruitment and receptor internalization(27).

Previous studies have demonstrated a role for β-arr1 and β-arr2 during myocardial ischemia. β-arr1 KO mice show improved cardiac function in a model of post–myocardial infarction HF. At this regard, the underlying mechanisms were referred to improved cardiac β-AR signaling and function due to cardiac β-Arr1 absence and, decreased circulating levels of cathecolamines and aldosterone due to adrenal β-Arr1 deletion(28). β-arr-2 KO mice have greater mortality compared to WT mice after MI and their infiltrated macrophages induce huge cardiac inflammation(29). Moreover, β-arr2 overexpression stimulate cardiac contractility and reduced LV dilation after MI via sarco[endo]plasmic reticulum Ca2+-ATPase (SERCA2a) increased activity(30). However, it is not been shown whether β-arr2 plays a role in age-dependent cardiac β-AR desensitization and functional decline.

Our study is the first indicating that β-arr2 deletion is able to induce a significant increase in cardiac function, as indicated by the significant improvement in LV EF and blunted age-related LV dilation observed in β-arr2 KO-Old compared to WT-Old (20-month-old) mice (Fig. 4 and Table). Importantly, the β-arr2 KO and WT mice showed similar cardiac parameters when young (6-month-old) (Fig.4 and Table). No difference was found in HW, HW/BW, HW/TL or LV Mass AW (Fig. 3-4; Table) suggesting that β-arr2 is not involved in hypertrophic response during aging.

Recently, echocardiographic speckle-Tracking based strain imaging has emerged as an accurate non-invasive tool for the evaluation of LV function and morphology in mouse models, beyond the standard measurements(16, 31). It has been shown that echocardiographic strain analysis is a valuable and reproducible technique both in elderly patients and mouse models of cardiac aging(31-33). Interestingly, we found that that β-arr2 deletion was able to counteract the decrease in radial strain parameters during aging. In fact, β-arr2 KO-Old mice showed increased both average radial strain and average radial SR when compared to WT-Old mice (Fig.5). In addition, differently from WT-Old mice, β-arr2 KO-Old mice preserved radial strain and radial SR in the anterior basal zone and posterior apex. No differences were found in terms of longitudinal strain or longitudinal SR between β-arr2 KO and WT mice both at 6- and 20-months time-point.

Interestingly, we found β-arr2 protein levels to be upregulated in aging heart while we did not find a difference in β-arr2 mRNA expression levels between in LV lysates from WT-Young and WT-Old mice (Fig. 1). Probably, β-arr2 transcript and protein expression decoupling is due to age-related post-translational regulations. At this regard, it is well known a decrease in total rates of protein degradation with age and β-arr ubiquitination has been shown to be regulated by different proteins such as parkin and Mdm2(34, 35).

In addition, our results indicate that β-arr2 deletion is not counterbalanced by β-arr1 upregulation in aged hearts. This is crucial since β-arrs have structural analogies and share several functions in GPCR regulation and GPCR-independent transduction signaling(36).

In order to check the molecular mechanism involved, we have measured cardiac β-AR density in β-arr2 KO and WT mice when young and old. β-AR altered responsiveness and signaling are recognized to be a relevant pathogenic mechanism for reduced LV function during aging in animal models and in humans(6). However, therapeutic interventions able to restore age-related cardiac β-AR abnormalities has not been found, yet. Our results showed that β-arr2 deletion was able to completely restore β-AR down-regulation with β-AR levels similar to those observed in young mice. Tang et al. confirmed the importance of β-AR pathway during aging and showed that the activation of cardiac Adenylyl Cyclase 6 expression, effector molecule for β-AR signaling, improved aging-related LV systolic and diastolic function through enhanced sarcoplasmic reticulum calcium uptake(23).

In our study, βarr-2 deletion induced results similar to those reported by Tang et colleagues, improving aging-impaired LV contractile function (Fig. 3-7). However, βarr-2 deletion should have more beneficial effect due to its multiple roles: 1) βarrs not only bind to GRK phosphorylated receptors to induce receptor internalization but also act as a scaffold protein

for numerous other molecules such as phosphodiesterase to further diminish β-AR-induced cAMP signal(37-39); 2) βarr-2 is involved in heterologous desensitization of βARs by other GPCR stimuli (such as dopamine or angiotensin II) which block β-adrenergic-induced protein kinase A phosphorylation of phospholamban and myocyte contractility.

This latter finding is particularly relevant taking into consideration the age-dependent increase of local renin-angiotensin system in the myocardium(40).

We believe that the different effects of β-arr-2 deletion during cardiac aging and post-ischemic HF are due to different cells and molecular mechanism involved. In fact, macrophage β-arr-2 plays a protective role in MI-induced inflammation while during aging β-arr-2 seems to be a crucial modulator of β-AR function in cardiomyocytes (Fig. 8)(29).

With age, the heart shows a decrease in the number of cardiomyocytes, increase in their size and in fibrotic areas. All these phenomena are related to the production of ROS during aging, which are considered to be of mitochondrial origin(41). Nox4 is a key enzyme in ROS production while Mn-SOD shows an anti-oxidant role(20). It has been demonstrated that Nox4 is upregulated during aging especially in the mitochondria and its overexpression induces cellular senescence in fibroblasts and apoptosis in cardiomyocytes(20). Intriguingly, Philip et al. have recently demonstrated that β-arrs are upregulated in cardiac fibroblasts from failing hearts and regulate mitochondrial superoxide production via Nox4(42). Our results show that β-arr2 is involved in age-dependent Nox-4 upregulation suggesting that reduced oxidative stress could improve, at least in part, cardiac function and remodeling in β-arr2 KO-Old compared to WT-Old mice (Fig. 9). Although additional studies will be required to determine whether global deletion of β-arr2 is beneficial for cardiac aging due to β-arr2 role in cardiomyocytes or in other cardiac cell populations, our current data suggest a therapeutic potential for β-arr2 inhibition in aging hearts.

CONCLUSIONS

In summary, the present study reports that β-arr2 deletion reverses age-related cardiac dysfunction and LV dilatation. Importantly, the beneficial effects of β-arr2 deletion were found in global and regional radial strain parameters. As a contributing mechanism, improved LV function is associated with restored β-AR density and reduced oxidative stress in aged hearts.

REFERENCES

1.   Mozaffarian D, Benjamin EJ, Go AS, Arnett DK, Blaha MJ, Cushman M, et al. Heart Disease and Stroke Statistics-2016 Update: A Report From the American Heart Association. Circulation. 2016;133(4):e38-360.

2.   Nakou ES, Parthenakis FI, Kallergis EM, Marketou ME, Nakos KS, Vardas PE. Healthy aging and myocardium: A complicated process with various effects in cardiac structure and physiology. Int J Cardiol. 2016;209:167-75.

3.   Lieber SC, Qiu H, Chen L, Shen YT, Hong C, Hunter WC, et al. Cardiac dysfunction in aging conscious rats: altered cardiac cytoskeletal proteins as a potential mechanism. Am J Physiol Heart Circ Physiol. 2008;295(2):H860-6.

4.   Scalia GM, Khoo SK, O'Neill S, Group LS. Age-related changes in heart function by serial echocardiography in women aged 40-80 years. J Womens Health (Larchmt). 2010;19(9):1741-5.

5.   North BJ, Sinclair DA. The intersection between aging and cardiovascular disease. Circ Res. 2012;110(8):1097-108.

6.   Ferrara N, Komici K, Corbi G, Pagano G, Furgi G, Rengo C, et al. β-adrenergic receptor responsiveness in aging heart and clinical implications. Front Physiol. 2014;4:396.

7.   Dai DF, Chen T, Johnson SC, Szeto H, Rabinovitch PS. Cardiac aging: from molecular mechanisms to significance in human health and disease. Antioxid Redox Signal. 2012;16(12):1492-526.

8.   Reiter E, Ahn S, Shukla AK, Lefkowitz RJ. Molecular mechanism of β-arrestin-biased agonism at seven-transmembrane receptors. Annu Rev Pharmacol Toxicol. 2012;52:179-97.

9.   Luttrell LM, Gesty-Palmer D. Beyond desensitization: physiological relevance of arrestin-dependent signaling. Pharmacol Rev. 2010;62(2):305-30.

10.   Sato PY, Chuprun JK, Schwartz M, Koch WJ. The evolving impact of g protein-coupled receptor kinases in cardiac health and disease. Physiol Rev. 2015;95(2):377-404.

11.   Leosco D, Rengo G, Iaccarino G, Filippelli A, Lymperopoulos A, Zincarelli C, et al. Exercise training and beta-blocker treatment ameliorate age-dependent impairment of beta-adrenergic receptor signaling and enhance cardiac responsiveness to adrenergic stimulation. Am J Physiol Heart Circ Physiol. 2007;293(3):H1596-603.

12.   Dobson JG, Fray J, Leonard JL, Pratt RE. Molecular mechanisms of reduced beta-adrenergic signaling in the aged heart as revealed by genomic profiling. Physiol Genomics. 2003;15(2):142-7.

13.   Bohn LM, Lefkowitz RJ, Gainetdinov RR, Peppel K, Caron MG, Lin FT. Enhanced morphine analgesia in mice lacking beta-arrestin 2. Science. 1999;286(5449):2495-8.

14.   Duran JM, Makarewich CA, Sharp TE, Starosta T, Zhu F, Hoffman NE, et al. Bone-derived stem cells repair the heart after myocardial infarction through transdifferentiation and paracrine signaling mechanisms. Circ Res. 2013;113(5):539-52.

15.   Cannavo A, Liccardo D, Eguchi A, Elliott KJ, Traynham CJ, Ibetti J, et al. Myocardial pathology induced by aldosterone is dependent on non-canonical activities of G protein-coupled receptor kinases. Nat Commun. 2016;7:10877.

16.   Bauer M, Cheng S, Jain M, Ngoy S, Theodoropoulos C, Trujillo A, et al. Echocardiographic speckle-tracking based strain imaging for rapid cardiovascular phenotyping in mice. Circ Res. 2011;108(8):908-16.

17.   Bauer M, Cheng S, Unno K, Lin FC, Liao R. Regional cardiac dysfunction and dyssynchrony in a murine model of afterload stress. PLoS One. 2013;8(4):e59915.

18.   Grisanti LA, Traynham CJ, Repas AA, Gao E, Koch WJ, Tilley DG. β2-Adrenergic receptor-dependent chemokine receptor 2 expression regulates leukocyte recruitment to the heart following acute injury. Proc Natl Acad Sci U S A. 2016;113(52):15126-31.

19.   Luan B, Zhao J, Wu H, Duan B, Shu G, Wang X, et al. Deficiency of a beta-arrestin-2 signal complex contributes to insulin resistance. Nature. 2009;457(7233):1146-9.

20.   Ago T, Matsushima S, Kuroda J, Zablocki D, Kitazono T, Sadoshima J. The NADPH oxidase Nox4 and aging in the heart. Aging (Albany NY). 2010;2(12):1012-6.

21.   Yazdanyar A, Newman AB. The burden of cardiovascular disease in the elderly: morbidity, mortality, and costs. Clin Geriatr Med. 2009;25(4):563-77, vii.

22.   Yancy CW, Jessup M, Bozkurt B, Butler J, Casey DE, Colvin MM, et al. 2017 ACC/AHA/HFSA Focused Update of the 2013 ACCF/AHA Guideline for the Management of Heart Failure: A Report of the American College of Cardiology/American Heart Association Task Force on Clinical Practice Guidelines and the Heart Failure Society of America. Circulation. 2017;136(6):e137-e61.

23.   Tang T, Hammond HK, Firth A, Yang Y, Gao MH, Yuan JX, et al. Adenylyl cyclase 6 improves calcium uptake and left ventricular function in aged hearts. J Am Coll Cardiol. 2011;57(18):1846-55.

24.   Xiao RP, Tomhave ED, Wang DJ, Ji X, Boluyt MO, Cheng H, et al. Age-associated reductions in cardiac beta1- and beta2-adrenergic responses without changes in inhibitory G proteins or receptor kinases. J Clin Invest. 1998;101(6):1273-82.

25. Leineweber K, Klapproth S, Beilfuss A, Silber RE, Heusch G, Philipp T, et al. Unchanged G-protein-coupled receptor kinase activity in the aging human heart. J Am Coll Cardiol. 2003;42(8):1487-92.

26. Ungerer M, Parruti G, Böhm M, Puzicha M, DeBlasi A, Erdmann E, et al. Expression of beta-arrestins and beta-adrenergic receptor kinases in the failing human heart. Circ Res. 1994;74(2):206-13.

27. Hinz L, Ahles A, Ruprecht B, Küster B, Engelhardt S. Two serines in the distal C-terminus of the human ß1-adrenoceptor determine ß-arrestin2 recruitment. PLoS One. 2017;12(5):e0176450.

28. Bathgate-Siryk A, Dabul S, Pandya K, Walklett K, Rengo G, Cannavo A, et al. Negative impact of β-arrestin-1 on post-myocardial infarction heart failure via cardiac and adrenal-dependent neurohormonal mechanisms. Hypertension. 2014;63(2):404-12.

29. Watari K, Nakaya M, Nishida M, Kim KM, Kurose H. β-arrestin2 in infiltrated macrophages inhibits excessive inflammation after myocardial infarction. PLoS One. 2013;8(7):e68351.

30. McCrink KA, Maning J, Vu A, Jafferjee M, Marrero C, Brill A, et al. β-Arrestin2 Improves Post-Myocardial Infarction Heart Failure via Sarco[endo]plasmic Reticulum Ca(2+)-ATPase-Dependent Positive Inotropy in Cardiomyocytes. Hypertension. 2017.

31. Koch SE, Haworth KJ, Robbins N, Smith MA, Lather N, Anjak A, et al. Age- and gender-related changes in ventricular performance in wild-type FVB/N mice as evaluated by conventional and vector velocity echocardiography imaging: a retrospective study. Ultrasound Med Biol. 2013;39(11):2034-43.

32. Li RJ, Yang J, Yang Y, Ma N, Jiang B, Sun QW, et al. Speckle tracking echocardiography in the diagnosis of early left ventricular systolic dysfunction in type II diabetic mice. BMC Cardiovasc Disord. 2014;14:141.

33. Xia JZ, Xia JY, Li G, Ma WY, Wang QQ. Left ventricular strain examination of different aged adults with 3D speckle tracking echocardiography. Echocardiography. 2014;31(3):335-9.

34. Martinez-Vicente M, Sovak G, Cuervo AM. Protein degradation and aging. Exp Gerontol. 2005;40(8-9):622-33.

35. Ahmed MR, Zhan X, Song X, Kook S, Gurevich VV, Gurevich EV. Ubiquitin ligase parkin promotes Mdm2-arrestin interaction but inhibits arrestin ubiquitination. Biochemistry. 2011;50(18):3749-63.

36.   Luttrell LM, Lefkowitz RJ. The role of beta-arrestins in the termination and transduction of G-protein-coupled receptor signals. J Cell Sci. 2002;115(Pt 3):455-65.

37.   Perry SJ, Lefkowitz RJ. Arresting developments in heptahelical receptor signaling and regulation. Trends Cell Biol. 2002;12(3):130-8.

38.   Perry SJ, Baillie GS, Kohout TA, McPhee I, Magiera MM, Ang KL, et al. Targeting of cyclic AMP degradation to beta 2-adrenergic receptors by beta-arrestins. Science. 2002;298(5594):834-6.

39.   Shi Q, Li M, Mika D, Fu Q, Kim S, Phan J, et al. Heterologous desensitization of cardiac β-adrenergic signal via hormone-induced βAR/arrestin/PDE4 complexes. Cardiovasc Res. 2017;113(6):656-70.

40.   Conti S, Cassis P, Benigni A. Aging and the renin-angiotensin system. Hypertension. 2012;60(4):878-83.

41.   Lesnefsky EJ, Chen Q, Hoppel CL. Mitochondrial Metabolism in Aging Heart. Circ Res. 2016;118(10):1593-611.

42.   Philip JL, Razzaque MA, Han M, Li J, Theccanat T, Xu X, et al. Regulation of mitochondrial oxidative stress by β-arrestins in cultured human cardiac fibroblasts. Dis Model Mech. 2015;8(12):1579-89.

FIGURES

Figure 1:

A

B

Figure 2:

A

B

Figure 3:

A Heart weight

B HW/BW

C HW/TL

WT
β-Arr2KO

Figure 4:

A Ejection Fraction

B Ejection Fraction

C LVIDd

D LVIDd

E LV Mass AW

F LV Mass AW
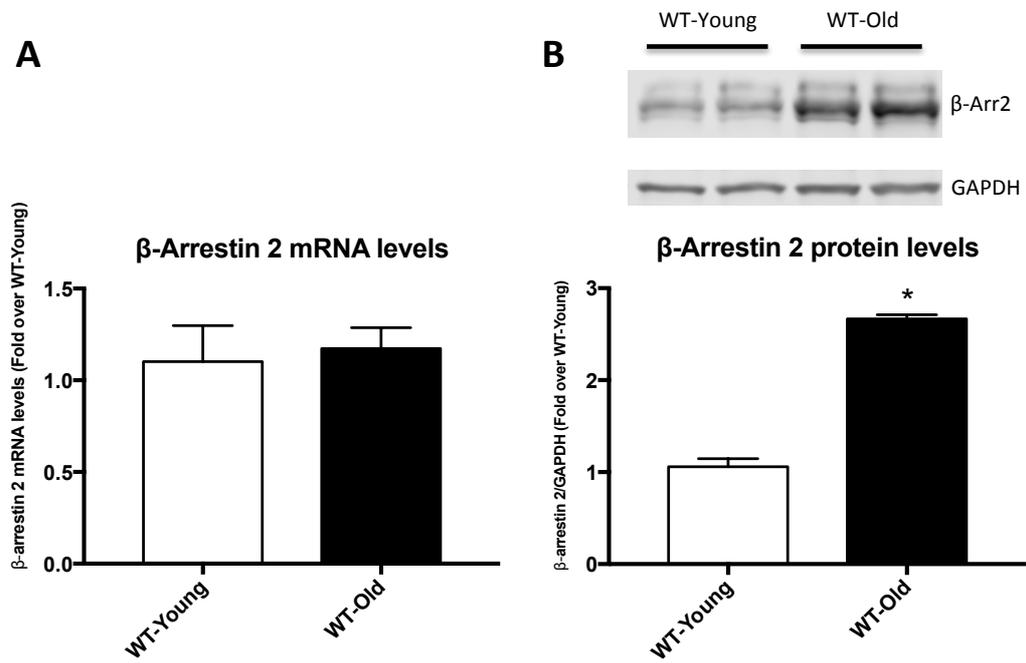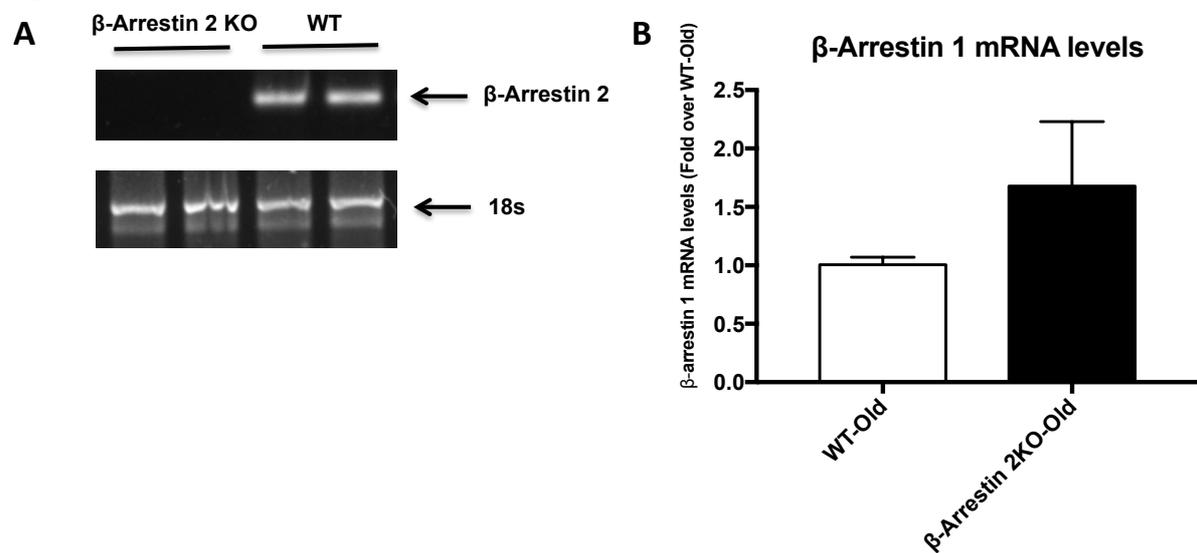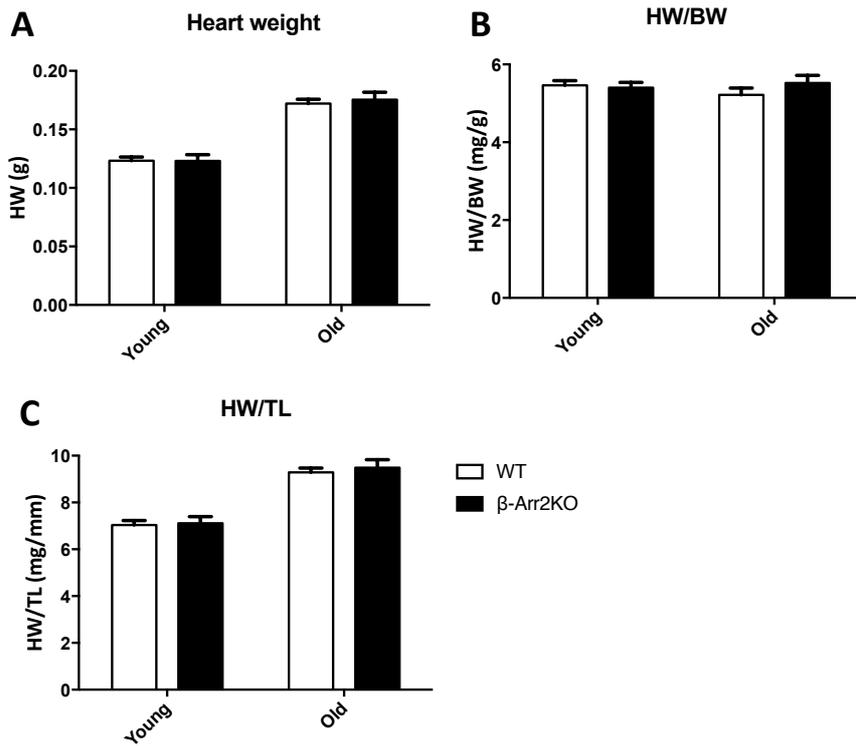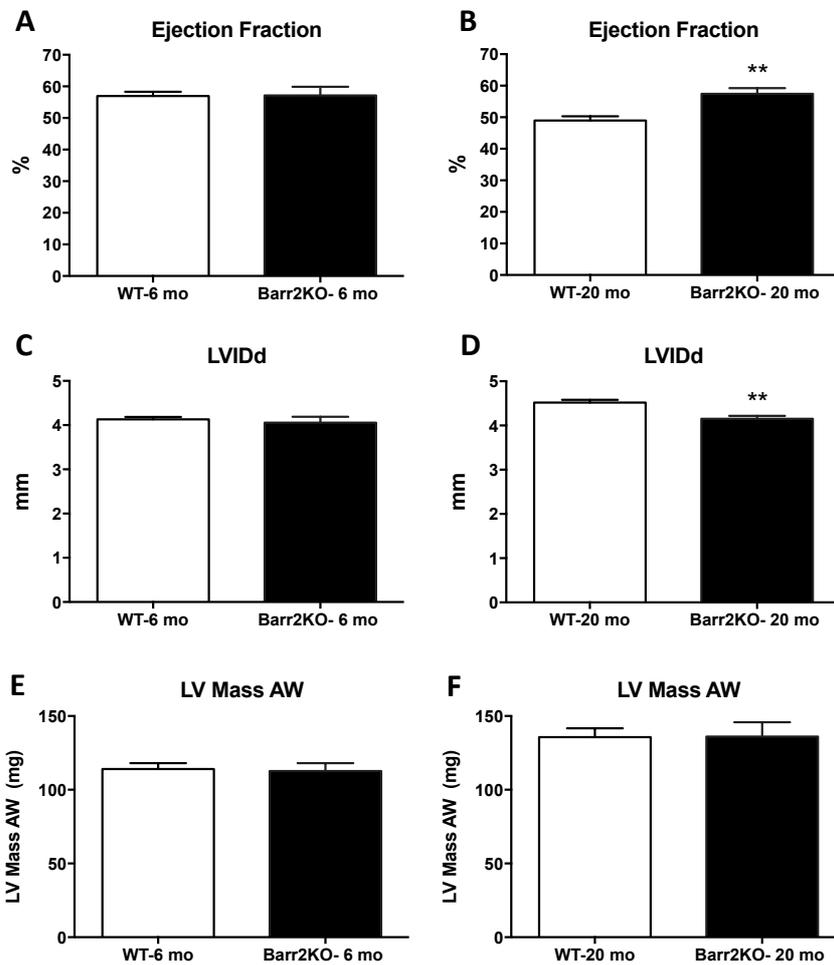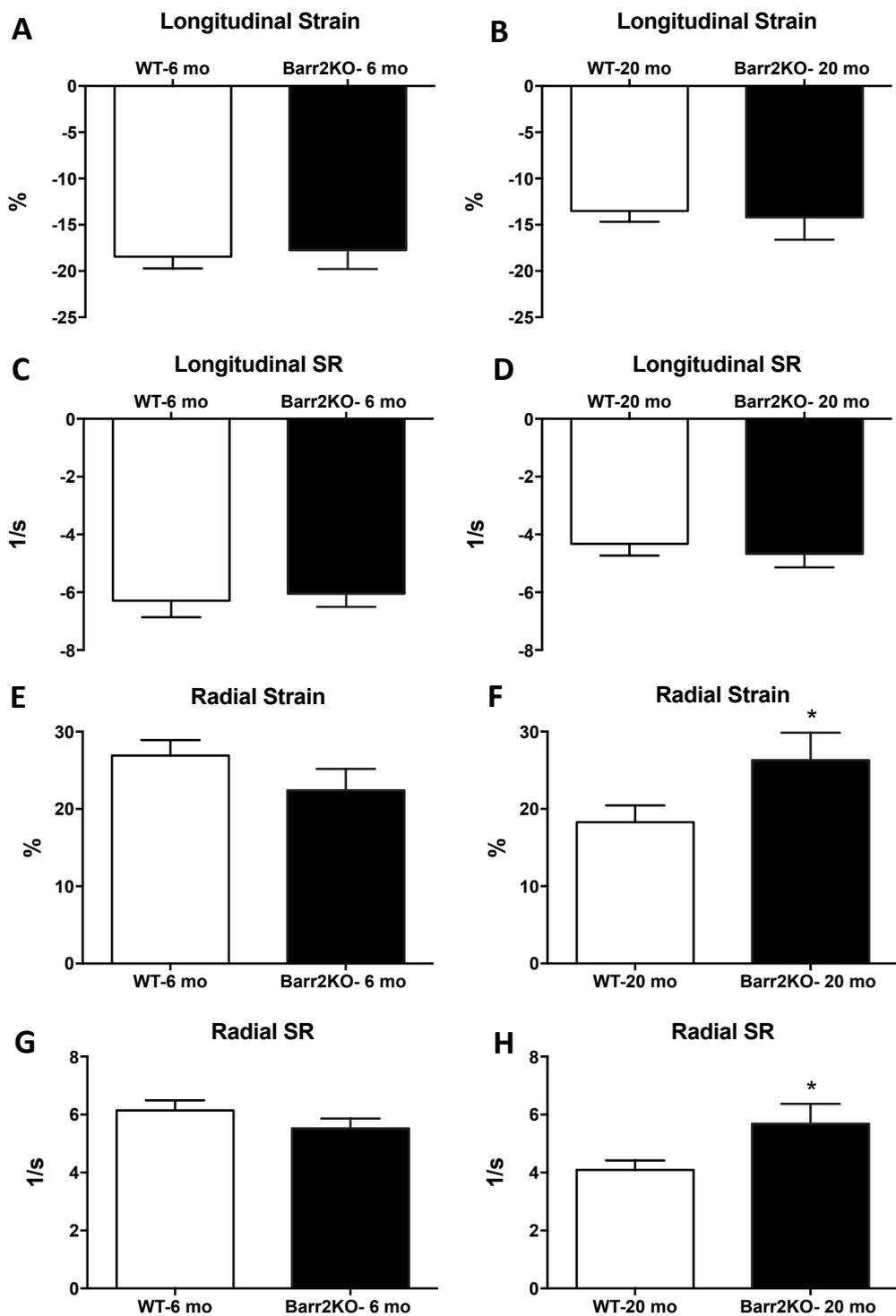
Figure 5:

Figure 6:

Figure 7:

Figure 8:

βAR density
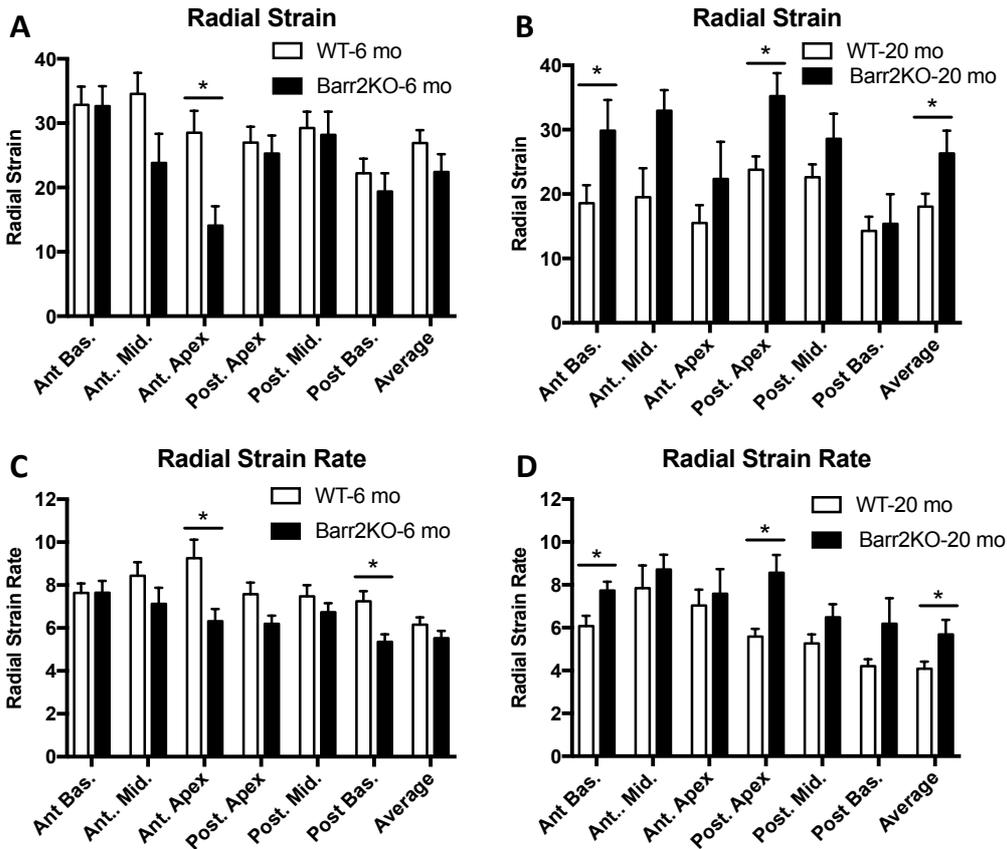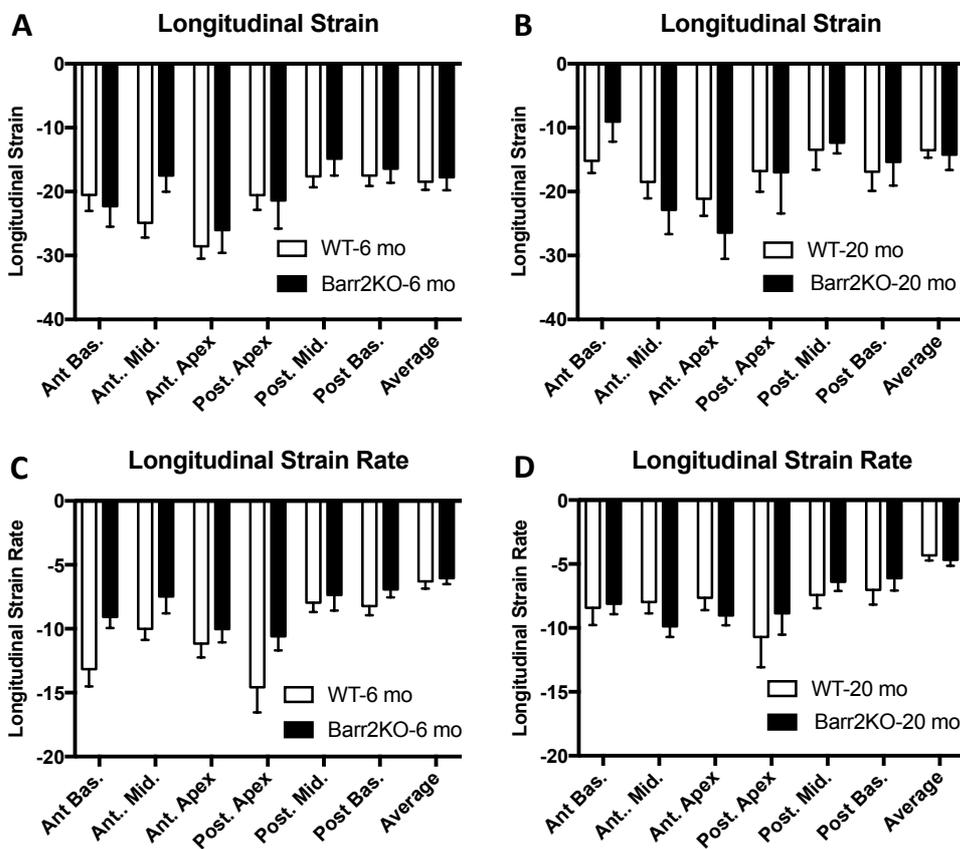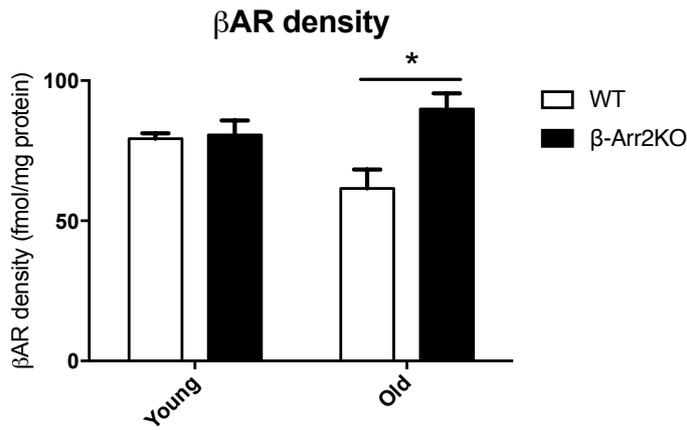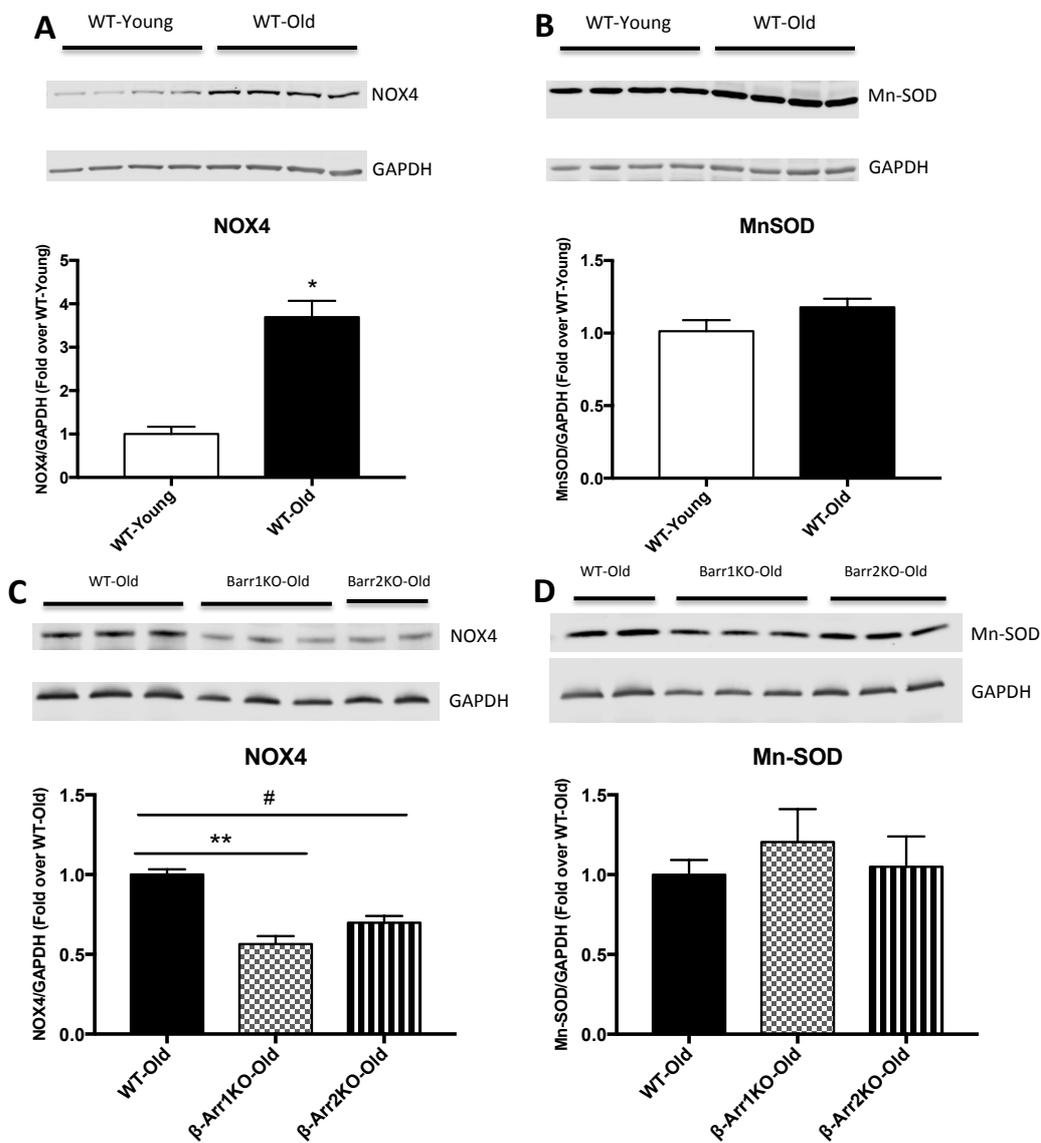
Figure 9:

FIGURE LEGENDS

Figure 1: Aging is associated with increased β-Arrestin 2 protein levels:

A: Quantification of RT-PCR data showing β-Arrestin 2 mRNA levels of left ventricular (LV) samples from WT-Young (3 months old) and WT-Old (15 months old) mice. Quantitation normalized with 18s as control and expressed as fold of WT-Young.

B: Representative Western blotting (top) and densitometric quantitation (bottom) in LV samples from WT-Young and WT-Old mice for β-Arrestin 2 . Representative blot shown includes GAPDH as loading control. Densitometric quantitation, normalized with GAPDH as control and expressed as fold of WT-Young. n= 4 to 5 per group. *, p<0.0001 vs WT-Young. T-test was used between groups.

Figure 2: β-Arrestin 2 deletion does not significantly alter β-Arrestin 1 expression during aging:

A: PCR in cardiac mRNA isolated from β-Arrestin 2 KO or WT mice for confirmation of the absence of β-Arrestin2 transcript. 18s used as control. **B:** Quantification of RT-PCR data showing β-Arrestin1 mRNA levels of left ventricular (LV) samples from WT-Old (15 months old) and β-Arrestin 2 KO-Old mice. Quantitation normalized with 18s as control and expressed as fold of WT-Old. n= 4 per group. T-test was used between groups.

Figure 3: β-Arrestin 2 deletion does not affect cardiac hypertrophy during aging:

Heart weight (HW) **(A)**, HW/body weight (HW/BW) **(B)** and HW/tibia length (HW/TL) **(C)** in WT and β-Arrestin 2 KO (β-Arr2KO) mice. Both mice have been studied when 3- (Young) and 24- (Old) -month-old. n= 6 to 26 per group. T-test was used between groups.

Figure 4: β-Arrestin 2 deletion ameliorates age-related cardiac dysfunction:

Ejection fraction (EF) **(A, B)**, left ventricular internal diameter at diastole (LVIDd) **(C, D)** and left ventricular mass of the anterior wall (LV Mass AW) **(E, F)** as measured by standard echocardiography in WT and β-Arrestin 2 KO (Barr2KO) mice. Both mice have been studied when 6- and 20-month-old (6-mo and 20-mo). n= 6 to 19 per group. **p<0.01 vs WT-20mo. T-test was used between groups.

Figure 5: β-Arrestin 2 deletion counteracts age-related radial strain dysfunction:

Average longitudinal strain **(A, B)**, longitudinal strain rate (SR) **(C, D),** radial strain **(E, F)** and radial SR **(G-H)** as measured by echocardiographic speckle-tracking based strain imaging in WT and β-Arrestin 2 KO (Barr2KO) mice. Both mice have been studied when 6- and 20-month-old (6-mo and 20-mo). n= 6 to 18 per group. *p<0.05 vs WT-20 mo. T-test was used between groups.

Figure 6: β-Arrestin 2 deletion improves segmental radial strain during aging:

Radial strain **(A, B)** and radial strain rate **(C, D)** for 6 different segments of left ventricle (anterior basal zone, anterior middle zone, anterior apex, posterior apex, posterior middle zone and posterior basal zone) as measured by echocardiographic speckle-tracking based strain imaging in WT and β-Arrestin 2 KO (Barr2KO) mice. Both mice have been studied when 6- and 20-month-old. n= 6 to 18 per group. *p<0.05. T-test was used between groups.

Figure 7: β-Arrestin 2 deletion does not affect segmental longitudinal strain during aging:

Longitudinal strain **(A, B)** and longitudinal strain rate **(C, D)** for 6 different segments of left ventricle (anterior basal zone, anterior middle zone, anterior apex, posterior apex, posterior middle zone and posterior basal zone) as measured by echocardiographic speckle-tracking

based strain imaging in WT and β-Arrestin 2 KO (Barr2KO) mice. Both mice have been studied when 6- and 20-month-old. n= 6 to 18 per group. T-test was used between groups.

Figure 8: β-Arrestin 2 deletion ameliorates age-related β-adrenergic receptor dysfunction:
β-adrenergic receptor (βAR) density (femtomoles of receptor per milligram of protein) in WT and β-Arrestin 2 KO (β-Arr2KO) mice. Both mice have been studied when 3- (Young) and 24- (old) month-old. n= 6 to 9 per group. *p<0.05. T-test was used between groups.

Figure 9: β-Arrestin 1 or 2 deletion ameliorate oxidative stress during aging:
Representative Western blotting (top) and densitometric quantitation (bottom) in left ventricle (LV) samples from WT-Young (3 months old) and WT-Old (15 months old) mice for NADPH oxidase 4 (NOX4) **(A)** and Manganese-dependent superoxide dismutase (MnSOD) **(B)**. Representative Western blotting and densitometric quantitation in LV samples from WT-, β-Arrestin 1KO (β-Arr1 KO)- and β-Arr2 KO- Old mice(15-month-old) for NOX4 **(C)** and MnSOD **(D)**. Densitometric quantitation, normalized with GAPDH as control and expressed as fold of WT-Young or WT-Old, as appropriate. n = 4 to 5 per group. *p<0.001 vs WT-Young. **p<0.0001 vs WT-Old; #p<0.01 vs WT-Old. T-test or One-way ANOVA and Tukey test were used between groups, as appropriate.

TABLE

	6-month-old mice			20-month-old mice		
	WT	**β-Arr 2 KO**	**p-value**	**WT**	**β-Arr 2 KO**	**p-value**
BW (g)	23±0.65	23±0.66	NS	33±0.87	32±0.79	NS
HW (g)	0.12±0.0032	0.12±0.0054	NS	0.17±0.0036	0.18±0.0063	NS
HW/BW (mg/g)	5.4±0.11	5.4±0.14	NS	5.2±0.18	5.5±0.2	NS
HW/TL (mg/mm)	7±0.19	7.1±0.28	NS	9.3±0.18	9.5±0.34	NS
HR (bpm)	492±8	462±13	NS	494±13	480±14	NS
EF (%)	57±1.3	57±2.7	NS	49±1.3	57±1.8**	<0.01
LVIDd (mm)	4.1±0.054	4.1±0.13	NS	4.5±0.066	4.2±0.067**	<0.01
LVIDs (mm)	3.0±0.053	3.0±0.15	NS	3.5±0.067	3.1±0.11**	<0.01
LVAWd (mm)	0.79±0.033	0.82±0.059	NS	0.76±0.029	0.89±0.052*	<0.05
LVAWs (mm)	1±0.037	1.1±0.063	NS	1.1±0.029	1.2±0.028	NS
LVPWd (mm)	0.72±0.02	0.7±0.022	NS	0.77±0.031	0.81±0.047	NS
LVPWs (mm)	0.98±0.035	1±0.043	NS	0.91±0.052	1.1±0.035*	<0.05
LV Mass AW	114±3.9	113±5.3	NS	136±6	136±9.7	NS

Table legend: Physical parameters and echocardiography measurements:
Body weight (BW), heart weight (HW), HW/BW, HW/tibia length (HW/TL), heart rate (HR), ejection fraction (EF), left ventricular internal diameter at diastole (LVIDd) and systole (LVIDs), anterior wall in diastole (LVAWd) and systole (LVAWs), posterior wall in diastole (LVPWd) and systole (LVPWs), and mass of the anterior wall (LV Mass AW) were evaluated in WT and β-Arrestin 2 KO (β-Arr2KO) mice. Both mice have been studied when 6- and 20-month-old. Values represent mean±SE. n=6 to 26 per group. *p<0.05 vs WT-20-month-old **p<0.01 vs WT-20-month-old. T-test was used between groups.